BUCKLING OF COMPOSITE SHELLS WITH GEOMETRIC IMPERFECTIONS

Chiara Bisagni

Dipartimento di Ingegneria Aerospaziale
Politecnico di Milano
Via Golgi 40, 20133 Milano, Italy
e-mail: chiara@aero.polimi.it

List of symbols

z	axial coordinate
ϑ	circumferential coordinate
L	cylinder's length
m	number of axial waves
n	number of circumferential waves
a	imperfection's amplitude
w	mean cylinder surface's shift
ε	adimensional imperfection's amplitude
λ	buckling load of the imperfect cylinder
λ_p	buckling load of the perfect cylinder
Λ	knock down factor

Abstract

The work presented in this paper is part of a research project aimed at improving the knowledge of the buckling phenomena of composite shells.
Particularly, the work addresses the experimental and numerical study of the effect of the geometric imperfections on the buckling behaviour of composite cylindrical shells under axial compression.
The experimental buckling tests have been performed on two series of composite cylinders under axial compression, by a loading rig controlled in position. The cylinders of two series have different types of lay-up orientation: cross-ply $(0°/90°)_s$ and angle-ply $(+45°/-45°)_s$. Each ply is made by kevlar cross-weaved fibres embedded into epoxy resin matrix. An ad-hoc equipment has allowed to measure the initial geometric imperfections and the buckling pattern development on the specimens internal surface.
The buckling behaviour is afterwards numerically investigated by means of the finite element code MARC. A non-linear analysis, with the finite element models including the geometric imperfections as well, has been performed for different values of the imperfection's amplitude. The first results of the numerical simulation of the experimental tests are below presented. The numerical models, validated by the experimental results, can be useful in a better understanding of the buckling phenomena and of the sensitivity with respect to the geometric imperfections, to properly define actually applicable strength design criteria.

Introduction

At present, the lack of generally applicable design criteria for composite structures is an important factor that inhibits the efficient use of composite materials in aerospace industrial applications, forcing the use of unduly high safety factors. The helicopters, where the weight saving is even more important than for fixed wing aircrafts, have been among the first flying machines adopting structural components made by composite materials. Some very important problems, such as fatigue in rotor blades, have been well identified and almost completely solved, while for others a solution seems not well indicated till now. This is particularly true in the case of buckling strength prediction of composite shell structures, where the geometric imperfections highly influence the buckling behaviour, producing discrepancies between the experimental results and the theoretical ones (Refs. 1,2). The effect is particularly severe in axially compressed cylindrical shells, where the presence of almost coincident buckling modes makes these structural elements more sensitive to the geometric imperfections (Refs. 3,4).
A combination of experimental, numerical and analytical activities is needed, to improve the knowledge of shells buckling phenomena, since the use of numerical simulations only cannot be accepted in place of expensive experimental programmes. The experimental tests are needed at least to validate the numerical and analytical models. These validated models can afterwards be useful to understand the critical factors that mainly influence the buckling phenomena and to study cases that are not

experimentally considered for practical reasons, allowing then to perform a wider parametric study essential for the definition of strength design criteria. The availability of well established design criteria will offer significant advantages in weight saving during the design of aerospace structures.

Specimen characteristics

The available specimens (Figure 1) are given by AGUSTA S.p.A and are characterised by the geometric properties reported in Table 1.

Table 1 - Geometric properties of the specimens.

Length *[mm]*	700
Radius *[mm]*	350
Thickness *[mm]*	1.04

They present two thicker reinforced ends at the top and bottom to facilitate the fixing into the loading rig. The actual length is therefore limited to the central part of the cylinder and is equal to 540 *mm*.

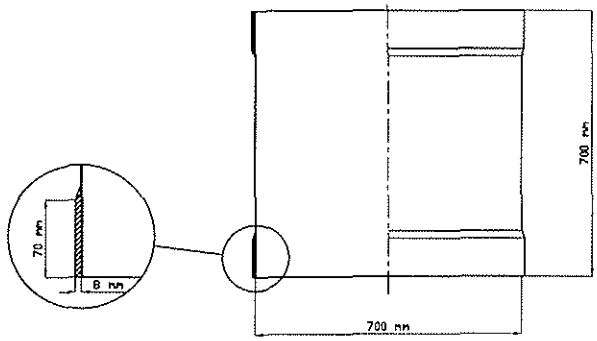

Figure 1 - Cylindrical specimen.

Each ply of the specimens is made by kevlar cross-weaved fibres embedded into epoxy resin matrix and has the structural properties reported in Table 2, where x_1 and x_2 are the orthogonal in-plane axes.

Table 2 - Structural properties of the specimens plies.

E_{11} *[N/mm²]*	23450
E_{22} *[N/mm²]*	23450
G_{12} *[N/mm²]*	1520
G_{13} *[N/mm²]*	1520
G_{23} *[N/mm²]*	1520
ν_{12}	0.2
ρ, density *[kg/mm³]*	1.32×10^{-6}
t, thickness *[mm]*	0.26

The tested specimens present two different types of lay-up orientation: cross-ply $(0°/90°)_S$ and angle-ply $(+45°/-45°)_S$.

Experimental tests

An extensive experimental program of buckling tests on the composite cylindrical shells under axial compression has been performed (Ref. 5). The possibility to test series of nominally identical specimens allows a deep study of the effect of the geometric imperfections on the buckling behaviour.

The test are performed by a loading rig, controlled in position. In fact, the axial load is provided by an hydraulic ram, but the actual load applied to the specimen is controlled, with a good accuracy, by four adjustable screw stops, acting on the four corners of the loading platform.

The compression load and the axial displacement respectively are measured, during the tests, by three load cells, located under the lower clamp, and by three LVDT transducers, measuring the distance between the two clamps.

An ad-hoc equipment (Figure 2) allows to measure the geometric imperfections and the buckling pattern development on the specimens internal surface (Ref. 6).

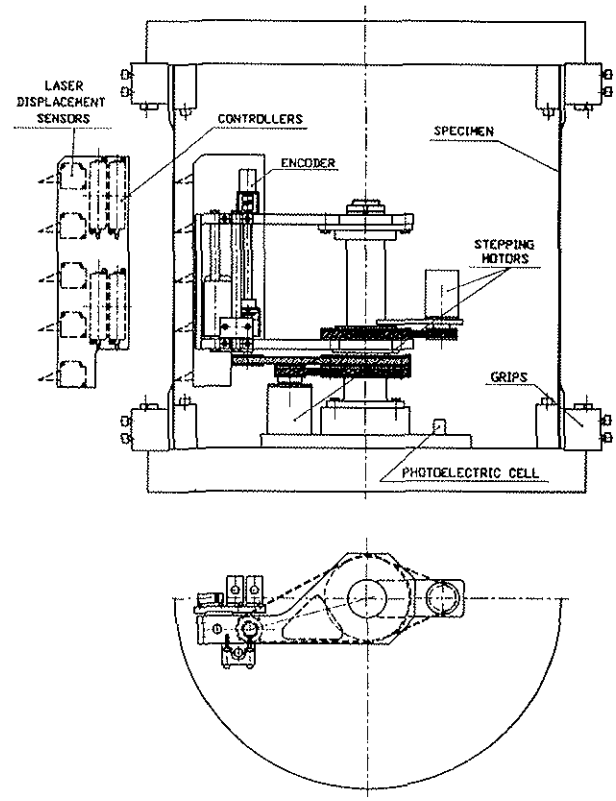

Figure 2 - Experimental equipment.

These measurements are obtained by five laser displacement sensors, fixed on a slide, capable to rotate and vertically translate. These movements are given by two stepping motors and allow to measure, with at least one laser sensor, all the points of the central part of the cylinder internal surface. This covered area is limited to 450 *mm*.

The vertical position of the slide is known by an incremental encoder. The laser displacement sensors are placed at the distance of 40 *mm* from the specimen internal surface. They offer a measurement range of ±10 *mm* with a resolution of 15 μ*m* allowing to record both the geometric imperfections (some tens of micrometers) and the buckling pattern (about 10 - 20 *mm*).
Table 3 reports the values of the buckling loads and the corresponding axial displacements, recorded during two different cross-ply cylinders tests and during two different angle-ply cylinder tests. They are compared to the values of the buckling loads obtained by theory.

Table 3 - Tests results and comparison between experimental and theoretical buckling loads.

	Experim. buckling load *[N]*	Axial displ. *[mm]*	Theoret. buckling load *[N]*	Experim./ Theoret. loads
C-ply	32706	0.315	37112	0.88
C-ply	32608	0.303	37112	0.87
A-ply	35640	1.557	37214	0.95
A-ply	35178	1.563	37214	0.94
C-ply = cross-ply A-ply = angle-ply				

While the buckling loads of the two different lay-up cylinders are in the same range of values, even if the difference between the experimental and the theoretical buckling load is smaller for the angle-ply cylinders than for the cross-ply ones, the axial displacements of the angle-ply cylinders assumes much larger values than those of the corresponding cross-ply cylinders. Figure 3 shows a typical diagram of the compression load versus the axial displacement for an angle-ply cylinder, where both loading and unloading sequences are reported.

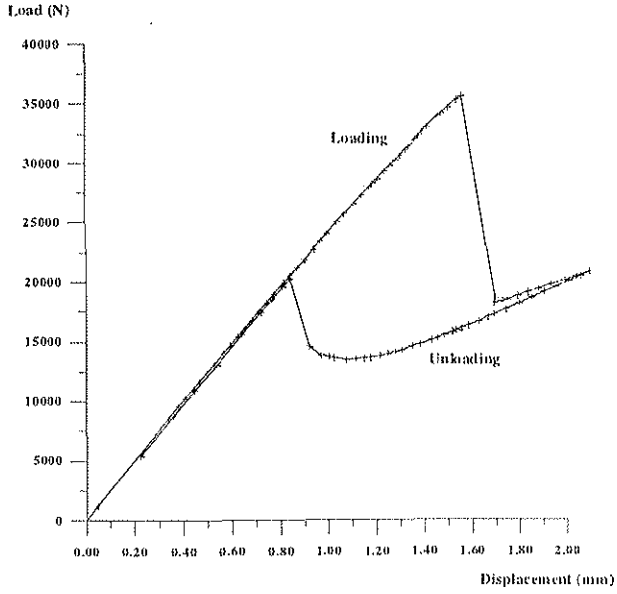

Figure 3 - Compression load versus axial displacement (angle-ply cylinder).

The equipment allows to record the cylinder's internal surface before the test, measuring the geometric imperfections, and about 15-20 times during the test itself; in fact the time required to measure a complete surface is limited to 4 minutes. The measurements are recorded in a regular mesh of points 10 *mm* spaced both circumferentially and axially.
During all the tests no differences are measured among the surfaces recorded during the pre-buckling.
A typical buckling pattern for a cross-ply cylinder is reported in Figure 4.

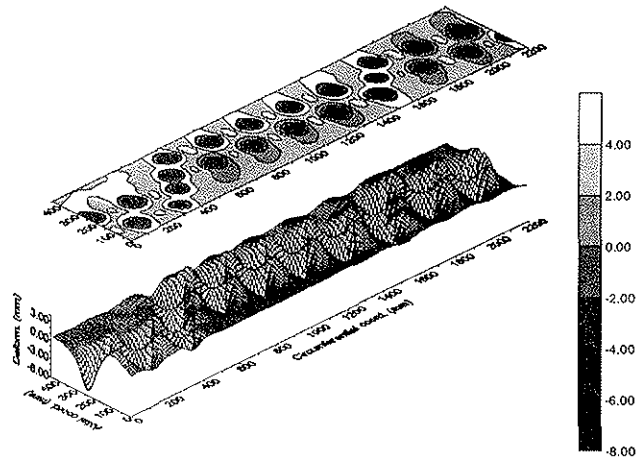

Figure 4 - Typical buckling pattern for a cross-ply cylinder.

There are about 11 circumferential waves and 2 axial waves. The pattern doesn't change significantly in postbuckling, where there is only a depth's growth. At the maximum cylinder axial displacement, the displacements normal to the surface reach 7 mm internally and 4 mm externally.
Figure 5 shows a typical buckling pattern for an angle-ply cylinder. The waves are here 8 circumferentially and only 1 axially and the displacement normal to the surface reaches 11 and 5 *mm* internally and externally respectively.

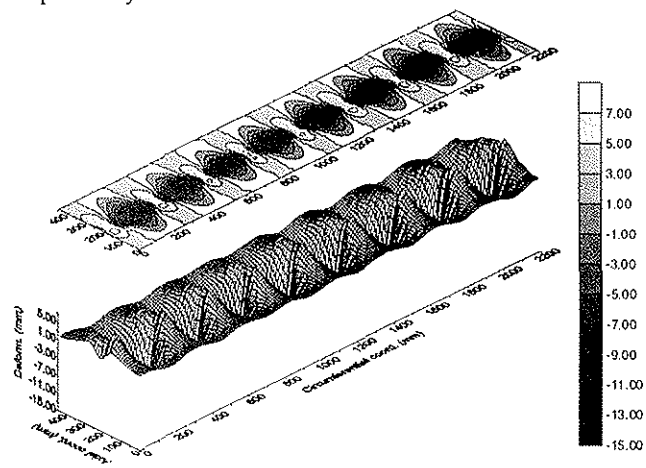

Figure 5-Typical buckling pattern for an angle-ply cylinder.

During all the tests the unloading is resulted always completely elastic.
In Figure 6 a photograph of a typical buckling pattern for a cross-ply cylinder, as it appears during the test, is reported.

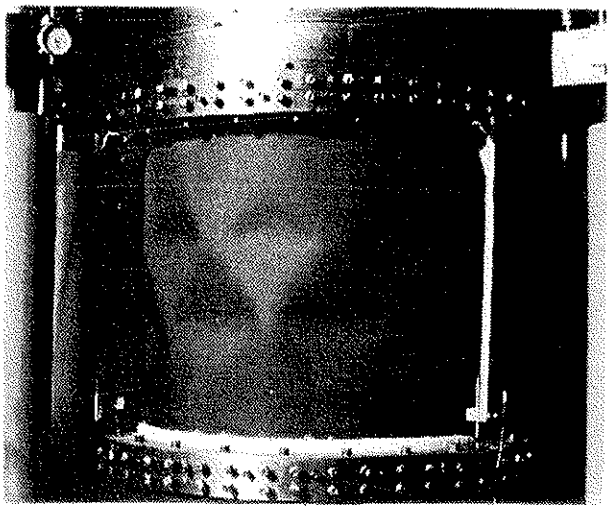

Figure 6 - Cross-ply cylinder under test.

Finite element analysis

The experimental activity is supported by a finite element analysis, aiming at the set-up of numerical models, having the same characteristics of the real specimens and able to reproduce the results of the experimental tests, i.e. both the buckling load values and the postbuckling behaviours. These validated models could be useful to understand the conditions that mainly influence the buckling phenomena and to study other cases not experimentally considered, allowing to perform a wider parametric study, fundamental in the definition of strength design criteria.
The analysis is done by the finite element code MARC (version K6.1). At first, a buckling eigenvalue analysis is performed. The cylinders are considered as perfect, without initial imperfections, to compare the results to the theoretical predictions. Because of the two thicker reinforced ends at the top and bottom of the cylindrical shells, the finite element model's length is taken equal to 560 *mm*. This value is equal to the length of the specimens central part, 540 *mm*, plus 10 *mm* for each part. The other geometric dimensions and the material properties are the same of the real shells.
The cylinders are modelled using 4-nodes bilinear shell elements, including transverse shear effects (MARC element 75). Other types of elements have been used, such as 8-nodes shell elements, but they did not give acceptable results.
The upper and lower ends of the considered cylinder are supposed to remain plane and circular, maintaining the initial radius. This is obtained by means of rigid links between every node at the two ends and two central fictitious nodes, one for each side of the cylinder. All the degrees of freedom on the central node of the lower end are eliminated by single point constraints, while the central node of the upper end can only translate along the axial direction.

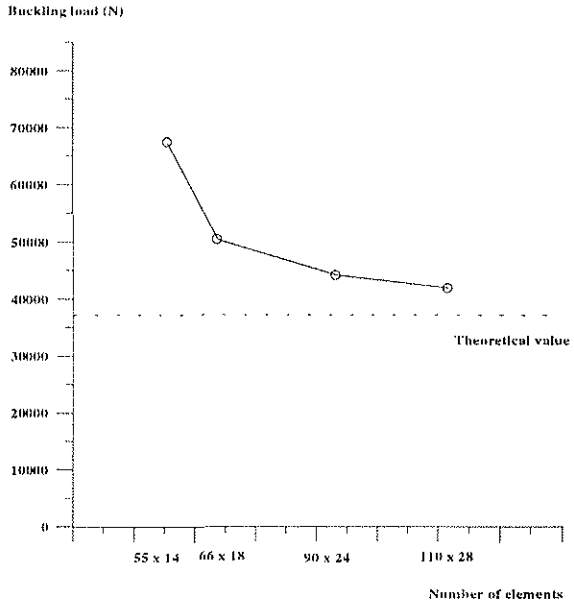

Figure 7 - Buckling load values for different meshes (cross-ply cylinder).

Figures 7 and 8 report the linear buckling loads of a cross-ply and of an angle-ply cylinder as obtained by the eigenvalue analysis with four different meshes, respectively of 55x14, 66x18, 90x24 and 110x28 circumferential by axial elements.

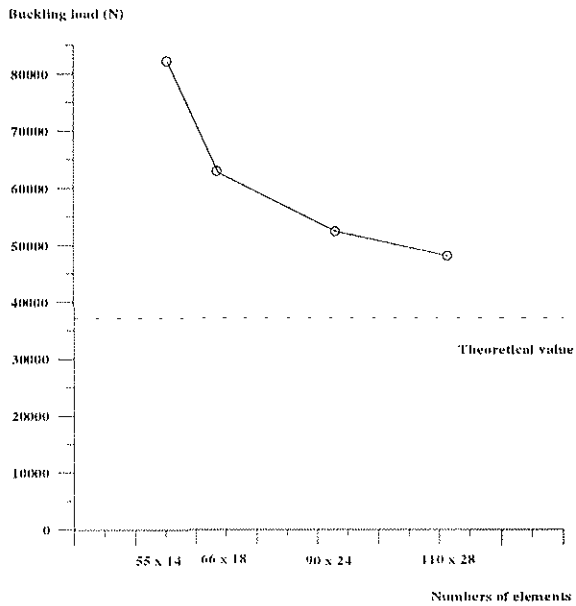

Figure 8 - Buckling load values for different meshes (angle-ply cylinder).

The resulting shell elements have the dimensions of 40x40, 33.33x31.11, 24.44x23.33 and 20x20 millimetres respectively.

In the case of mesh with 110x28 elements the difference between the so calculated linear buckling load of a cross-ply cylinder (41850 *N*) and the theoretical value (37112 *N*) is less than 11%, while for an angle-ply cylinder the calculated linear buckling load (48050 *N*) is different from the theoretical value (37214 *N*) for 22%.
The buckling pattern of the cylinders without geometric imperfections depends on the lay-up orientation. The cross-ply cylinder presents an asymmetric mode, with 13 circumferential waves and 4 axial waves (Figure 9), while the angle-ply cylinder presents an axialsymmetric mode with 7 axial waves (Figure 10).

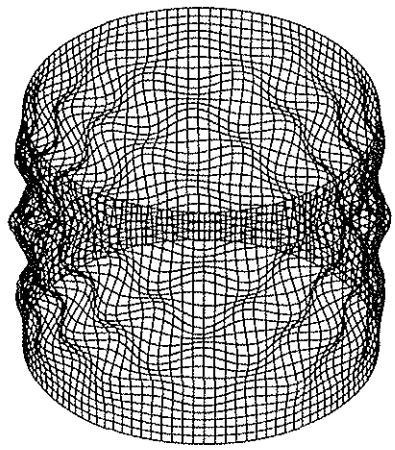

Figure 9 - Numerical buckling pattern for a cross-ply cylinder.

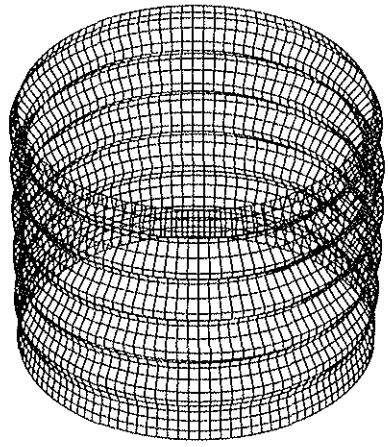

Figure 10 - Numerical buckling pattern for an angle-ply cylinder.

The values of the linear buckling loads, obtained by an eigenvalue analysis, can be considered as a good approximation of the ultimate load. But in the study of the postbuckling behaviour of the composite cylindrical shells under axial compression, the strains, that remain elastic, are not small and then a non-linear analysis must be performed (Ref. 7). A path-following algorithm with displacement control is used. In this non-linear analysis the buckling load is identified in correspondence of the first maximum in the load-displacement curve. In some cases, the computational effort to reach this point step by step can be, in term of CPU time, very expensive. The non-linear buckling loads for axially compressed composite cylinders, using a mesh composed by 110x28 elements, are reported in Table 4.

Table 4 - Comparison between the buckling loads obtained by theory and by linear and non linear analysis.

	Theory [N]	Linear eigenvalue analysis [N]	Non-linear eigenvalue analysis [N]	Mode
C-ply	37112	41850	41760	Asymm.
A-ply	37214	48040	45090	Axisymm.
C-ply = cross-ply A-ply = angle-ply				

As expected, the buckling load calculated by the non-linear analysis is always slightly smaller than the corresponding linear eigenvalue analysis load.

Effect of geometric imperfections

The effect of the geometric imperfections on the buckling load of composite cylindrical shells under axial compression is here studied. Actually, in consequence of the technological process for obtaining the composite shells, many types of imperfections, such as thickness' variations, local delaminations, can appear in the real specimens. Particularly, many papers can be found in the literature, concerning the buckling load sensitivity with respect to the thickness variations (Ref. 8-11).
The main purpose of the present work is to investigate the influence on the buckling load of a local variation of the cylinder's diameter, i.e. a shift of the mean surface of the imperfect cylinder from that of the perfect one, due for example to an incorrect lamination.
This geometrical imperfection presents the following shape:

$$w(z,\vartheta) = a \sin(m\pi z/L)\cos(n\vartheta)$$

where:

z = axial coordinate
ϑ = circumferential coordinate
m = number of axial waves
n = number of circumferential waves
a = imperfection's amplitude
L = cylinder's length

A non-linear analysis is performed for different combinations of numbers of axial and circumferential waves. The ratio between the buckling loads obtained for the imperfect cylinders λ and those of the corresponding perfect cylinders λ_p is called *knock-down factor* (in the

following indicated as Λ) and it is an index of the sensitivity of the buckling load with respect to the considered geometrical imperfections.
For each combination of numbers of axial and circumferential waves, the analysis is performed for different values of the imperfection amplitude. The knock-down factor Λ changes significantly with the imperfection amplitude. In accordance with the Koiter's imperfection sensitivity theory (Ref. 12), the most critical imperfections present a shape similar to the buckling mode of the perfect cylinder.
The analysis results of a geometric imperfection characterized by 13 circumferential and 4 axial waves, applied both to cross-ply and angle-ply cylinder, are presented below. The analysis has been performed using 8 different values for the adimensional imperfection's amplitude ε, here defined as:

$$\varepsilon = a/t$$

(t = 1.04 *mm*) assuming the following values:

ε= 0 - 0.01 - 0.05 - 0.125 - 0.25 - 0.50 - 0.75 - 1.00

The non-linear buckling loads and the corresponding axial displacements are reported in Table 5, while the obtained knock-down factors are summarized in Table 6.

Table 5 - Buckling loads and axial displacements for the considered imperfections amplitudes.

ε	Buckling load *[N]* C-ply	Axial displ. *[mm]* C-ply	Buckling load *[N]* A-ply	Axial displ. *[mm]* A-ply
.000	41760	.430	45090	2.100
.010	40482	.443	43484	2.177
.050	38574	.465	41639	2.274
.125	35973	.499	38255	2.475
.250	31775	.565	31276	3.028
.500	31772	.565	31150	3.040
.750	31770	.565	30973	3.057
1.00	31765	.565	30765	3.078
C-ply = cross-ply A-ply = angle-ply				

Table 6 - Knock-down factors.

ε	Λ C-ply	Λ A-ply
.000	1.0000	1.0000
.010	0.9694	0.9644
.050	0.9237	0.9235
.125	0.8614	0.8484
.250	0.7609	0.6936
.500	0.7608	0.6908
.750	0.7607	0.6869
1.00	0.7606	0.6823
C-ply = cross-ply A-ply = angle-ply		

The same results are graphically represented in Figure 11 where the knock-down factors versus the imperfection's amplitude, for the cross-ply and the angle-ply cylinders respectively, are reported.

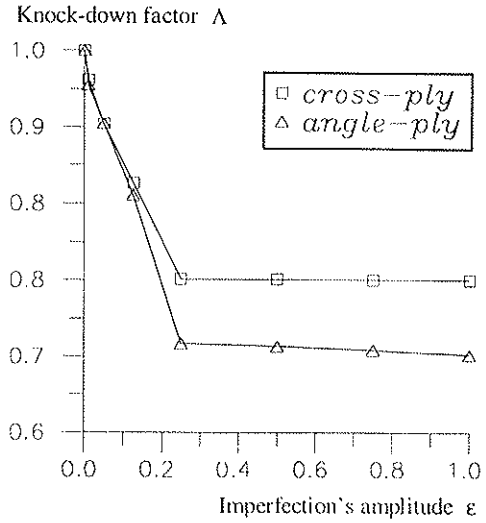

Figure 11 - Knock-down factors versus the imperfections amplitude: numerical results.

Looking at the resulting curves it appears that with the increasing of the imperfections amplitude the buckling loads decrease, both for the angle-ply and the cross-ply cylinders, with different slopes (greater in the case of angle-play layout) till a value of ε around 0.25. After that, the buckling loads don't change significantly.

Numerical simulation of the experimental tests

The imperfections measured on the real specimens before the buckling tests are introduced into the finite element model as a shift of the perfect cylinders surface.
The imperfections experimentally measured are recorded in a regular mesh of points 10 *mm* spaced both circumferentially and axially. Because of the computer limits, only a mesh of points 20 *mm* spaced can be used in the finite element model, obtaining the 110x28 elements mesh. The experimental imperfection measurements is unfortunately limited to the central part of the cylinders surface and the covered area has a length of 450 *mm*. In the finite element models, in the zones over and below this central part, the shift of the perfect cylinder is assumed as a linear variation from the imperfections measured at the limit of this central part to null imperfections in correspondence to the upper and lower ends of the cylinder. Table 7 reports the non-linear buckling loads obtained by the numerical simulations of two different cross-ply cylinder tests and two different angle-ply tests. A direct comparison cannot be done at this time since the numerical models must be corrected and validated by other kind of experimental results. The

finite element results, for example, seem to overestimate the post-buckling loads of the imperfect cylinders. In fact, in the case of experimental results, the values of the postbuckling loads of the perfect cylinders are not available, so the numerical overestimation could be simply related to a bad estimation of the structural stiffness, due to an incorrect evaluation of the material properties.

Table 7 - Comparison between experimental, theoretical and numerical buckling loads.

	Experim. buckling load [N]	Theoret. buckling load [N]	Numerical buckling load [N]
C-ply	32706	37112	39994
C-ply	32608	37112	35600
A-ply	35640	37214	40786
A-ply	35178	37214	39156
C-ply = cross-ply A-ply = angle-ply			

Unfortunately, because of great instabilities of the solution, the finite element code is not able to completely follow, in postbuckling, the curve indicating the variation of the axial reaction force versus the imposed displacement. The analysis stops not long after the maximum of that curve, defining the buckling load.

Conclusions

The first results of an experimental and numerical study of the effect of the geometric imperfections on the buckling behaviour of composite cylindrical shells have been presented. Experimental buckling tests have been performed on two series of composite cylinders under axial compression, by a loading rig controlled in position. An ad hoc equipment has allowed to measure the initial geometric imperfections and the buckling pattern development on the specimens internal surface.
The experimental activity has been supported by a numerical analysis using the finite element code MARC. The first results of the numerical simulation of the experimental tests have been here presented. The numerical models must be still improved and validated by other experimental tests, concerning different load conditions, such as torsion and combinations of axial compression and torsion, and concerning specimens with different lay-up configurations and made by different composite materials.
These models will allow to perform a wider study on the effect of the geometric imperfections and of the other parameters that mainly influence the buckling behaviour.

References

1. Kollar L., Dulacska E., *Buckling of shells for engineers*, John Wiley & Sons, 1984

2. Jullien J.F., *Buckling of shell structures on land, in the sea and in the air*, Lyon Symposium, Elsevier Applied Science, 1991

3. Jun S.M. and Hond C.S., *Buckling behaviour of laminated composite cylindrical panels under axial compression*, Computers and Structures, 1988.

4. Giavotto V., Poggi C. and Chryssanthopoulos M., *Buckling of imperfect composite shells under compression and torsion*, Proc. of Int. Meeting on Rotorcraft Basic Research, Atlanta, 1991.

5. Bisagni C., *Buckling and post-buckling behaviour of composite cylindrical shells*, Proceedings of XX ICAS Congress, Sorrento, 1996.

6. Bisagni C., *Instabilità di gusci cilindrici in materiale composito*, Proc. of AIDAA - XIII National Congress, Roma, 1995.

7. Hughes T.J.R., *The finite element methods: non-linear static and dynamic finite element analysis*, Prentice-Hall, 1987.

8. Cohen G.A., *Effect of a Nonlinear Prebuckling State on the Postbuckling Behavior and Imperfections Sensitivity of Elastic Structures*, AIAA Journal, vol.6 N.8, august 1968.

9. Cohen G.A. and Haftka, R.T., *Sensitivity of Buckling Loads of Anisotropic Shells of Revolution to Geometric Imperfections and Design Changes*, Computers & Structures, vol.31 N.6, 1989.

10. Koiter, W.T., Elishakoff I., Li, Y.W. and Starnes J.H.Jr., *Buckling of Axially Compression Imperfect Cylindrical Shells of variable Thickness*, Proceedings of 35th AIAA/ASME/ASCE/AHS/ASC Structures, Structural Dynamics and Materials Conf., Hilton Head, SC, 1994.

11. Li, Y.W., Elishakoff, I. and Starnes J.H.Jr., *Axial Buckling of Composite Cylindrical Shells with Periodic Thickness Variation*, Computers & Structures, vol.56 N.1, 1995.

12. Koiter W.T., A translation of *The stability of elastic equilibrium*, Technical Report AFFDL-TR-70 25, 1970.